REVIEW ARTICLE

SYNTHESIS AND APPLICATION OF SILVER NANOPARTICLES AS Fe²⁺ AND Mn²⁺ METAL-IONS CONTAMINANT REMOVAL MEDIA IN GROUNDWATER SAMPLES

Francis Nsiah, Isaac K. Attatsi, Michael K. Danquah and David K. Dodoo

Department of Chemistry, School of Physical Sciences, University of Cape Coast, Cape Coast, Ghana

ABSTRACT

The interest in the application of nanomaterials has been the focus of a number of scientific investigations in recent times. This drive has resulted mainly from the ease of synthesis, large surface area for adsorption, and tunable surface chemistry and functionalization of these nanomaterials. In this work, silver nanoparticles were synthesized and employed as metal–ion contaminant removal media for Mn^{2+} and Fe^{2+} in groundwater from the Cape Coast Metropolis. The nanoparticles were synthesized using reduction method. A bathochromic shift of the UV-vis absorbance measurements was used as an indication of physisorption onto the silver nanoparticles. A bathochromic shift from 400 to 440 nm from adsorption of Mn^{2+} and 400 to 460 for Fe^{2+} respectively onto silver nanoparticles were observed. Adsorption characteristics of the nanoparticles were evaluated at various incubation periods by observing the bathochromic shift and hypochromic effect in the absorption bands of the metal ions. The amount of metal ions removed through the application of the nanoparticles to standard solutions after fourteen days incubation were iron: 60–88% and manganese: 96–99%, whereas the highest removal efficiencies in groundwater wells were 41.02 for iron and 46.03 for manganese. It was found that the metal concentrations reduced as the incubation periods were increased.

KEY WORDS: Silver nanoparticles, Adsorption, Groundwater.

INTRODUCTION

A number of heavy metal contaminants such as lead, iron, manganese and cobalt have had adverse effect on water quality globally (Abdul Jameel, Sirajudeen, and Abdul vahith, 2012). However, improving water quality is a difficult task in areas where the risk of contamination is high (Pradeep and Anshup, 2009). Technologies that have been employed in water treatment include ion exchange, reverse osmosis, reduction, precipitation, and membrane filtrations. The major setback for most of these technologies have stemmed from their high operational and maintenance cost (Weng, Sharma, and Chu, 2008). According to Monteagudo *et al*. sludge disposal is another problem with most of these techniques (Monteagudo and Ortiz, 2000; Suksabye, Thiravetyan, and Nakbanpote, 2008). Nanotechnology is currently being used in several ways to improve water quality. The major factor which defines the capability of nanoparticles as an extremely versatile remediation tool is their very small particle sizes (1–100 nm). Nanoparticles can also be magnetized, which allows them to be attached to heavy metals. In addition, nanoparticles can be attached onto solid matrix such as activated carbon for improved water treatment (Ashutosh and Himanshu, 2010). In recent times, nanoparticles-based adsorption techniques have become versatile method for removal of metallic pollutants from aqueous solutions (Elangovan, Philip, and Chandraraj, 2008). This technique has been so effective that it removes metallic ions even at very low concentrations (Kogan *et al*., 2006; Shim and Gupta, 2007). Tremendous attention has been focused on the application of nanostructured materials as adsorbents or catalyst in the removal of removetoxic and

harmful substances from wastewater and air (Ding *et al*., 2005; Yang, Zhu, and Xing, 2006). Reactive nanoparticles appear to be useful in remediating groundwater and thus may prove useful in removing pesticides, herbicides and heavy metals in the environment (Ashutosh and Himanshu, 2010). This research presented herein explores the viability of the use of metal nanoparticles in the removal of metal-ion contaminants in groundwater samples in the Cape Coast Metropolis. The approach adopted in this work involves the synthesis and characterization of silver nanoparticles. The synthetic scheme employed in this work renders the NPs monodispersed in solution. This step is then followed by a proof of concept experiment where the efficacy of these nanoparticles was tested using standard solutions of Fe (II) and Mn (II) during varying periods of incubation. The final stage of this study focuses on the application and analysis of groundwater samples from five communities in the Cape Coast Metropolitan area. The concentrations of the metal-ions were compared with the EPA and the World Health Organization's stipulated standards.

EXPERIMENTAL SECTION

Description of study areas

The study areas located within the Cape Coast Metropolis lied within longitude 1° 11' 41" W and latitude 5° 07' 20" N in the coastal areas of the Central Region of Ghana as shown in Figure 1. A control sample was taken from Assin Fosu in the Assin North district of the Central Region which lies within longitude 1° 25' 41" W and latitude 6° 05' 20" N of the Central Region of Ghana. The control sample taken from inland served to ascertain the veracity of pollution of groundwater by sea water intrusion.

*Corresponding author: Francis Nsiah
Department of Chemistry, School of Physical Sciences, University of Cape Coast, Cape Coast, Ghana
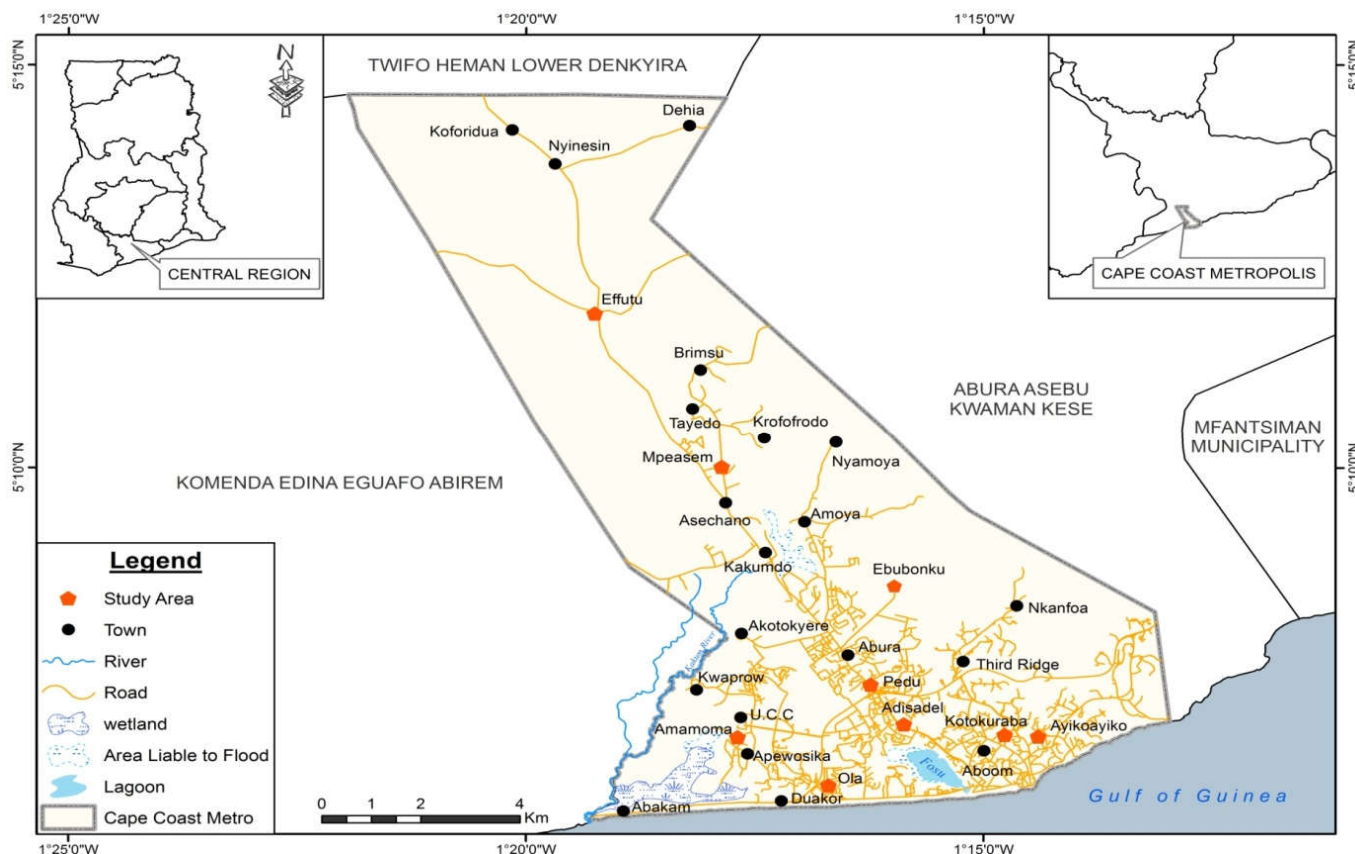
Figure 1. Map showing the areas of study in the Cape Coast Metropolis

All samples were taken from groundwater/wells which were the main source of water supply for the people within the communities. However, these wells were positioned in areas which could permit elevated levels of heavy metals to leach or deposit into them. The wells were also relatively close to automobile refurbishing shops, some major roads serving the communities, lorry parks and metal scrap dealing centres.

Sample collection, treatment and storage

The samples were collected from groundwater wells at five (5) sampling sites. The four (4) sites sampled within the Cape Coast Metropolis included Kotokuraba, Efutu, OLA and Pedu, and one control sample from Assin Fosu in the Assin North district of the Central Region of Ghana. Concentrated nitric acid treated 1 L polyethylene bottles were used for sampling to prevent traces of metals leaching into the water samples (*Standard Methods for the Examination of Water and Wastewater*, 2005).

In addition, the nitric acid treatment procedure was intended for the preservation of trace metals through the minimization of precipitation processes, microbial activity and adsorption losses to the walls of the sample container (Biziuk, Beyer, and Zukowska, 2010; Donald, Shugar, Shari, and Lauber, 2001; Sundaram *et al*., 2009). The measured temperature values for the samples ranged between 29–30°C with their corresponding pH values between 6.0 and 6.5 pH units. Samples were transported to the laboratory, and refrigerated at 4°C to minimize sample evaporation losses and any possible chemical transformation (*Standard Methods for the Examination of Water and Wastewater*, 2005).

Reagents and Materials

The UV–vis spectra were recorded on a T70 UV–vis spectrophotometer (PG Instrument Ltd.) with samples in a quartz cuvette. Varian 715–ES ICP-OES was employed for the quantitative analysis of amounts of iron (Fe^{2+}) and manganese (Mn^{2+}) ions removed from solution through the adsorption of the metal ions onto the nanoparticles surface. All chemicals were purchased from Merck (Darmstadt, Germany) and were of analytical reagent grade. All solutions were prepared using deionized water. A 0.005 M 1,10–phenanthroline, 0.001 M $AgNO_3$, and 0.002 M $NaBH_4$ solutions were prepared by dissolving the appropriate amount in 100 mL of deionized water. A special mercuric sulphate–silver nitrate solution was prepared by dissolving carefully weighed 15 g mercuric sulphate in a nitric acid solution to a 50 mL volume. A 50 mL portion of 85% phosphoric acid was added followed by 9 mg silver nitrate. The solution was then diluted to 250 mL and stored in an amber bottle to prevent any possible interference from sunlight.

Synthesis of silver nanoparticles (AgNPs)

20 nm silver nanoparticles sols employed in this study were synthesized following the method proposed by Solomon *et al*. (Solomon *et al*., 2007). The method involved the reduction of Ag^+ to Ag^0 based on dropwise addition of 0.001 M $AgNO_3$ to 0.002 M sodium borohydride with continuous stirring for about 20 min on an ice bath. Silver nanoparticles formation was observed by a change in the colour of the mixture from colourless to yellow. The presence of a colloidal suspension was detected by the reflection of a laser beam from the

particles (Solomon *et al.*, 2007). The equation for the synthesis is shown in equation (1) below:

$$AgNO_3 + NaBH_4 \longrightarrow Ag + {}^1/_2H_2 + {}^1/_2B_2H_6 + NaNO_3 \quad (1)$$
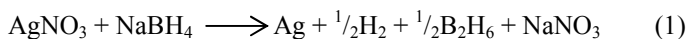
Preparation of sample blank

In the preparation of the blank solution, 100 mL distilled water was measured into a 125 mL Erlenmeyer flask followed by the addition of a 5 mL analytical grade concentrated nitric acid. The mixture was concentrated to about 15–20 mL volume with continuous addition of 2 mL portions of concentrated nitric acid until digestion was complete. The final volume of the sample was 100 mL through quantitative transfer. The morphology of the nanoparticles was analyzed using a scanning electron microscope S4800 FE-SEM system (Hitachi Scientific Equipment, Japan) equipped with an ultrahigh resolution, low voltage 10 kV SEM inspection with advanced sample navigation package.

Preparation of standard iron complex and manganese solutions

Phenanthroline method which involves the reduction of Fe (III) to Fe (II) state using hydroxylamine hydrochloride and 1, 10–phenanthroline as reducing and complexation agents respectively, was employed as stated elsewhere.(*Standard Methods for the Examination of Water and Wastewater*, 2005) Rapid dark orange colour development during the process was indicative of the presence of an excess of phenanthroline. 10, 20, 30, 40 and 50 mL portions of the iron stock solution were pipetted to prepare standard iron solutions of 2, 4, 6, 8 and 10 μg/mL in a 100 mL volumetric flask. The absorbance measurements were taken at 510 nm wavelength. Persulphate oxidation of soluble manganese compounds to form permanganate was carried out in the presence of silver nitrate.(*Standard Methods for the Examination of Water and Wastewater*, 2005) For spectrophotometric determination of manganese, 20, 40, 60, 80 and 100 mL portions of the manganese stock solution were pipetted to prepare standard manganese solutions of 2, 4, 6, 8 and 10 μg/mL to 100 mL final solution volume. Absorbance measurements were taken at 525 nm wavelength.

Treatment of standard iron and manganese solutions with AgNPs

2 mL portions of AgNPs sol were added to 10 mL portions of iron complex and manganese solutions. Different sets of the nanoparticles impregnated solutions from each standard iron complex and manganese were analyzed after 1 day, 3 days, 5 days, 7 days and 14 days incubation periods with the silver nanoparticle sols. Each solution was centrifuged at 3000 rpm for 10 min and the supernatant portions taken for UV–vis analysis. Absorbance measurements were taken at 510 nm for iron complex and 525 nm for manganese standard solutions, respectively. Deionised water was used as reference in each case and the absorbance values corrected with a reagent blank.

Groundwater sample treatment with AgNPs

Groundwater samples, on the other hand, were treated in two different ways. The first sets of samples (10 mL portions of each sample) were analyzed without the addition of any nanoparticles. The second sets of 10 mL portions of groundwater samples were treated with 2 mL portions of silver nanoparticles sols and incubated for various times. Incubation periods of 1 day, 3 days, 5 days, 7 days and 14 days similar to those of the standard solutions as described earlier in this manuscript were employed. Samples were centrifuged at 3000 rpm for 10 min. UV–vis absorbance measurements were taken at 510 nm for iron and 525 nm for manganese, respectively. Quantitative determinations of metal ion concentrations were carried out subsequent to UV-vis analysis using inductively coupled plasma-optical emission spectrophotometer (ICP–OES). This procedure was undertaken with a view to ascertain in comparative terms the amounts of iron (Fe^{2+}) and manganese (Mn^{2+}) ions removed through the adsorption of the metal ions onto the surfaces of AgNPs. The selected ICP–OES emission wavelengths for iron and manganese were 238.2 and 257.6 nm respectively.

RESULTS AND DISCUSSION

Characterization of Ag nanoparticles

Characteristically, noble metal nanoparticles (NPs) demonstrate strong absorption band in the UV-vis portion of the electromagnetic spectrum which is not present in the spectrum of the bulk metal. The absorption band results when the incident photon frequency is in resonance with the combined oscillation of the conduction electrons called the surface plasmons. The energy of the surface plasmon is responsive to the dielectric function of the material, the surrounding, the shape, and the size of the NPs. This responsive energy of the surface plasmon implies that if a metal ion attaches itself to the surface of a nanoparticles, the surface plasmon energy of the NP changes. The major thrust behind the application of UV–vis in this work is to detect wavelength shifts upon surface modification of the NPs. The UV–vis absorption spectra in the range of 300–700 nm for 20 nm AgNPs is shown in Figure 2. The 20 nm AgNPs showed distinctive surface plasmon absorption peaks at 406 nm, a characteristic of AgNPs. As the metal nanoparticle size increases and or upon surface adsorption, the plasmon band experiences a bathochromic shift. The absence of absorption peak at wavelengths greater than 600 nm indicated their well dispersed state in solution. AgNPs were further analyzed by SEM analysis of the colloidal gold solution. SEM image of AgNPs (Figure 3) showed particles of small sizes (20.3 ± 0.8 nm) with spherical shapes.
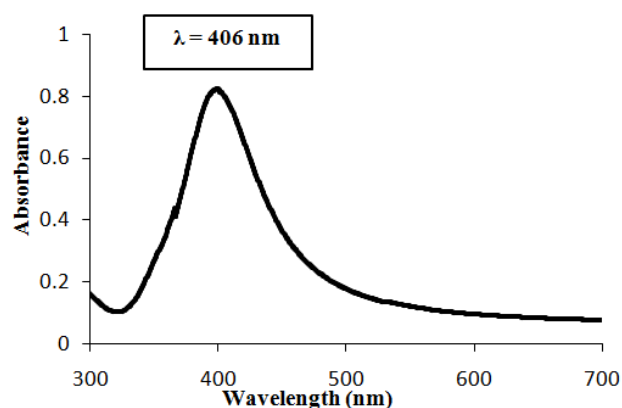
Figure 2. UV-Vis absorption spectrum for unmodified 20 nm AgNPs
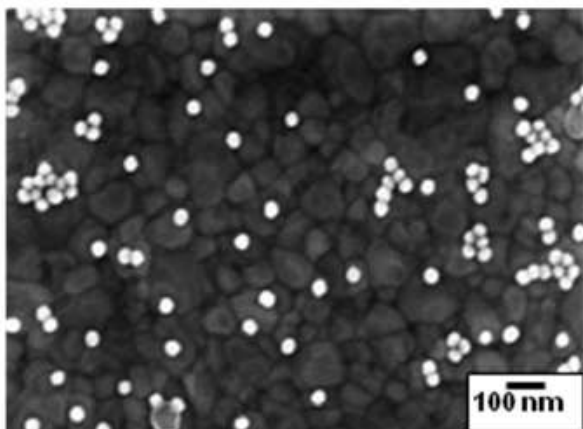
Figure 3. Scanning electron micrograph of 20 nm AgNPs

Effects of metal-ion adsorption on silver nanoparticles surface plasmon band

Subsequent to a successful synthesis and characterization of AgNPs, alterations in the surface plasmon band (SPB) of the NPs upon surface modification were examined. To ascertain shift in the plasmon band upon surface modification, a proof of concept experiment was carried out. In this experiment, about 2 mL of AgNPs was added to about 10 mL iron and manganese solution. The addition was made in the absence of the chelating agents and incubated for 1 h. The interaction between the metal ions and the NPs was based on physisorption within the solution pH range of 6–8 pH units. The sodium borohydride used in the synthesis of AgNPs reduced Ag^+ to Ag^0, and as well formed a negatively charged ionic sphere of borohydride ions around the NPs. The positively charged metal ions adsorbed to the surface of the NPs through their interactions with the surrounding negatively charged borohydride ionic sphere. Due to the far-reaching claims that have been made regarding the potential application of nanotechnology to groundwater treatment, it is essential to explore the basis for the adsorption of metal–ion contaminants onto AgNPs.

Figure 4 shows the shift patterns observed upon the interaction between the iron and manganese solutions, and the nanoparticles sols. We observed a significant red–shift from 406 to 460 nm upon the adsorption of iron (II) ions onto the surface of AgNPs. The adsorption of manganese (II) ions onto the nanoparticles, on the other hand, resulted in a relatively lower bathochromic shift from 406 to 440 nm than Fe^{2+} ion adsorption, as indicated in Figure 4. The shifts in the absorption maxima (λ_{max}) in Figure 4 indicate changes in the optical properties of the nanoparticles following the adsorption of iron and manganese ions. In addition, as indicated in Figure 4, there were marked hypochromic shifts of 0.822 to 0.439 a.u. for iron solution and 0.822 to 0.502 a.u. for manganese respectively. These decreases in absorbance intensities represent differences of 0.341 and 0.320 a.u. for Fe^{2+} and Mn^{2+} ions, respectively. It must be stated however that increased concentration of adsorbent species suggests an expansion of the diffused layer leading to an increase of the hydration sphere and the hydrodynamic radius of the nanoparticles. The results presented in this section further suggest that UV–vis spectrophotometry is a powerful technique for tracking the changes in optical properties of NPs upon surface modification. This proof of concept experiment provides the

foundation for the exploration into the effectiveness of nanoparticles in the removal of metal-ion contaminants from groundwater samples within the World Health Organisation (WHO) recommendable potable water pH range of 6–8 pH units.
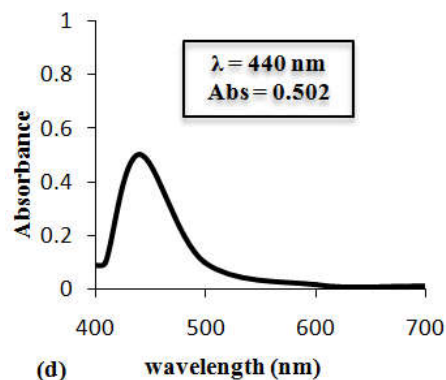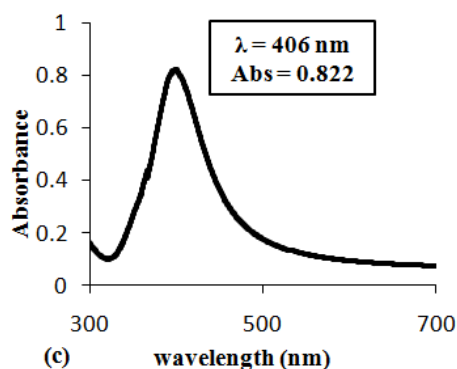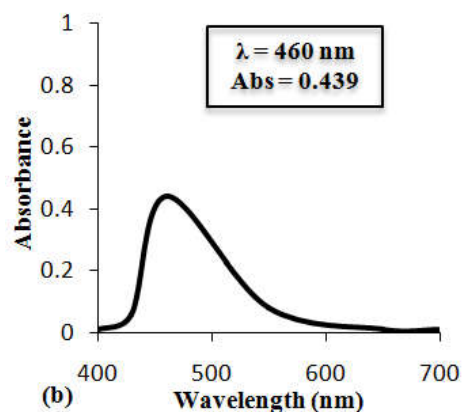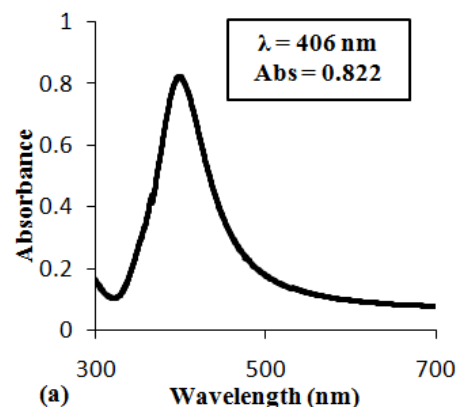
Figure 4. UV-Vis absorption spectra for 20 nm AgNPs (a and c) and bathochromic and hypochromic shift upon adsorption of iron and manganese solution to AgNPs (b and d)

Efficiency of AgNPs as metal-ion contaminant removal media

In order to employ the AgNPs in the groundwater treatment, it is essential to test their efficacy with variable standard solution concentrations of iron and manganese. It is worth mentioning that metals in potable water are predominantly found in their various oxidation states, some of which are best removed through complexation reaction with a chelating agent (*Standard Methods for the Examination of Water and Wastewater*, 2005; Sumesh, Bootharaju, Anshup, and Pradeep, 2011; Yantasee *et al*., 2007). In this study, we evaluated the effectiveness of adsorption capacities of nanoparticles as metal-ion contaminant removal media using various metal–ion solution concentrations with a fixed AgNP dosage. The investigation focussed on the physisorption of Fe^{2+} and Mn^{2+} ions onto the surfaces of the AgNPs from solution. Again, UV–vis absorption spectroscopy is a simple technique to explore the structural changes of molecules and to recognize the complex formation between different chemical entities. Hence, the absorption spectra of standard solutions of iron and manganese having bulk solution concentration range of 2–10 µg/mL in the presence of AgNPs were incubated from day 1 to day 14 were recorded and shown in Table 1.

and Mn^{2+} which are known water contaminants. The absorbance values measured at 510 and 525 nm for iron and manganese respectively were converted to percentages. The percentage removal of each metal ion was calculated using equation below and shown in Tables 2 and 3.

$$\% \, M^{n+} \text{removed} = \frac{(\text{Absorbance before NP addition} - \text{Absorbance after NP addition})}{\text{Absorbance before NP addition}} * 100 \% \quad (2)$$

The spectra obtained from the UV–vis measurements indicated that the absorbance values recorded for Fe^{2+} and Mn^{2+} solutions decreased with longer incubation periods which is indicates greater adsorption of metal-ion to the surface of the nanoparticles. As indicated in Table 1, adsorption of Fe^{2+} ions from solution on day 1 and day 3 showed a sharp decrease in absorbance for the 2 µg/mL solution. This observation reveals a rapid growth in adsorption even at short incubation periods. Generally, there was a decreasing trend in the absorbance measurements from day 1 to day 14 for the various range of concentrations employed in this work. This observation is consistent with the studies conducted by Alissawi *et al*. and Alqudami *et al*. which confirmed that metal ion adsorption to

Table 1. Absorbance of Fe (II) complex solutions at 510 nm using AgNPs. Absorbance measurements reported are the average values for 3 measurements and the standard deviations of all the spectral measurements were lower than 0.003 a.u.

Fe (II) conc. (µg/mL)	Before AgNPs addition	Day 1	Day 3	Day 5	Day 7	Day 14
2	0.0784	0.0751	0.0391	0.0240	0.0104	0.0094
4	0.2000	0.1273	0.1117	0.0923	0.0697	0.0690
6	0.3113	0.1893	0.1453	0.1415	0.1332	0.1330
8	0.4399	0.2141	0.2008	0.1998	0.1788	0.1785
10	0.5453	0.2647	0.2520	0.2444	0.2199	0.2160

Table 2. Percent of Fe (II) removed by AgNPs in different Fe (II) complex solutions incubated with AgNPs at different times. All values reported here on the average have standard deviations below ± 0.05%

Fe (II) conc. (µg/mL)	Abs before AgNPs addition	Day 1	Day 3	Day 5	Day 7	Day 14
2	0.078	4.21	50.13	69.39	86.73	88.01
4	0.200	36.35	44.15	53.85	65.15	65.50
6	0.311	39.19	53.32	54.55	57.21	57.28
8	0.440	51.33	54.35	54.58	59.35	59.42
10	0.545	51.45	53.78	55.18	59.67	60.39

Table 3. Percent (%) of Mn (II) removed by AgNPs in different Mn (II) complex solutions incubated with AgNPs at different times. All values reported here on the average have standard deviations below ± 0.05%

Mn (II) conc. (µg/mL)	Abs before AgNPs addition	Day 1	Day 3	Day 5	Day 7	Day 14
2	0.184	63.09	92.21	99.40	99.40	99.40
4	0.377	33.06	76.83	98.75	99.55	99.64
6	0.614	45.19	64.60	85.79	97.43	99.63
8	0.840	43.53	57.45	74.09	85.88	99.58
10	1.009	41.06	49.87	67.30	79.61	96.89

As discussed earlier in this manuscript, the adsorption of iron and manganese ions to the surface of AgNPs could result in the decrease of the absorbance intensities at 510 and 525 nm respectively, indicative of iron and manganese ion removal (Sumesh *et al*., 2011). The decrease in absorbance intensities depicts a decrease in concentration consistent with Beer-Lambert's law (Ball, 2006), which is interpreted as the removal of iron and manganese from solution. Again, the decrease in absorbance bears direct correlation with increase in the incubation period increases. Changes in the absorbance values were employed semi-quantitatively to establish the effectiveness of AgNPs in adsorbing metal ions such as Fe^{2+}

nanoparticles is time-dependent (Alissawi, Zaporojtchenko, Strunskus, Kocabas, and Chakravadhanula, 2013; Alqudami, Munassar, and Alhemiary, 2013). The data presented in Table 2 show the percentage Fe^{2+} ions adsorbed from 2 µg/mL solution on day 1 as 4.21%. On the other hand, day 14 recorded as high as 88.01% Fe^{2+} ions adsorbed from solution for the same solution concentration. The high percent removal on day 14 is as a result of the long incubation period.(Alissawi *et al*., 2013; Alqudami *et al*., 2013) It suffices to state from the results presented in Table 2 that adsorption of Fe^{2+} ions from solution increased steadily during 24 h of incubation in going

from 2 µg/mL to 10 µg/mL solutions. This result suggests that significant metal ion adsorption to nanoparticles can be achieved within shorter incubation periods even in the absence of surface modification or the anchorage of a capping agent. Apart from the rapid rate of adsorption observed in 2 µg/mL solution within the various periods of incubation, all other concentrations did not show sharp increase in Fe^{2+} ion adsorption from 24 h incubation to day 14. These minor changes in rate of adsorption for increasing incubation times might invoke electric double layer effect induced changes, which will require further investigations beyond the scope of this manuscript.

In effect, we want to reiterate the fact that effective Fe^{2+} metal-ion adsorption progresses from shorter to longer incubation times at less concentrated media. Table 3 shows the results from the Mn^{2+} ion adsorption after various periods of incubation for the range of 2–10 µg/mL Mn^{2+} solutions. It is interesting to note that adsorption from 2 µg/mL Mn^{2+} ion concentration within 24 h incubation resulted in 63.09% Mn^{2+} ion removal; which far higher than the amount of Fe^{2+} ions removed from solution under similar conditions. The lower percentage observed in the case of Fe^{2+} might be attributable to the structural arrangement posed by the phenanthroline–Fe^{2+} complex resulting in fewer Fe^{2+} ions within the hydration sphere around the nanoparticles surface. On the contrary, the persulphate procedure adopted in this study does not involve any complexing agent, hence direct adsorption of Mn^{2+} ions leading to its higher percent removal. The same reason might be assigned to the higher percent removal efficiencies (roughly 99.40%) observed for longer incubation periods for the same concentration. Again, this trend could imply that the nanoparticle adsorption efficiency reaches saturation after day 3 of incubation. Concentrations of 4, 6, 8 and 10 µg/mL on day 1 recorded 33.06, 45.19, 43.53 and 41.06% respectively. This indicates AgNPs adsorption begins immediately after addition to the Mn metal-ion solution. On the day 14, the same concentrations in their respective order recorded 99.64, 99.63, 99.58, 96.89%. This high percentage removal recorded on the day 14 also confirms the time–dependence of nanoparticles adsorption of metals in aqueous media.(Alissawi *et al.*, 2013; Alqudami *et al.*, 2013). The results presented in this confirm AgNPs as potential candidates for the removal of metal ion contaminants from water samples.

Quantitative determination of Fe^{2+} and Mn^{2+} ions in groundwater samples

As part of the objectives of this study, there was the need to apply a methodology to help quantify amounts of Fe^{2+} and Mn^{2+} metal ions removed from selected wells within the sampling sites. Since metal ions in groundwater samples are in trace amounts, ICP–OES was employed in the quantitative determinations of these metal ions. Five (5) samples which were not treated with AgNPs were first analyzed using ICP–OES to provide a baseline for comparison with the twenty–five (25) AgNP–treated groundwater samples. Table 4 shows the atomic emission results of the groundwater samples which were not treated with AgNPs prior to ICP–OES analysis. The results displayed in Table 4 show the highest concentrations for both Fe^{2+} and Mn^{2+} ions to be 0.581 (Pedu) and 0.299 (Kotokuraba) ppm respectively. The value recorded from Pedu is well above the permissible WHO iron concentration of 0.300

ppm for potable water (*Standard Methods for the Examination of Water and Wastewater*, 2005). Possible reasons attributable to this unusually high iron concentration from Pedu might be due to some leachates from nearby automobile repair shops and plausible pollution from vehicular movements within its vicinity. The transport mechanism with regard to this particular well would require further investigation beyond the scope of this paper. On the contrary, results obtained for manganese were all below the recommended WHO value of 0.500 ppm for potable groundwater samples, indicating no manganese pollution. It is worthy to note that only Kotokuraba recorded a lower iron (II) concentration than the control sample taken from Assin Foso. However, within the limits of experimental errors, only Kotokuraba and Efutu showed higher manganese concentrations than that recorded for Assin Foso. These results suggest that metal ion intrusions from the sea might have very little or no effect on the detectable metal ions levels obtained from these groundwater samples. Table 5, on the other hand, shows the percentage metal ion concentration remove from the groundwater samples relative to the concentrations shown in Table 4 after centrifugation following the AgNP treatment for various incubation periods. The periods for metal ion adsorption onto the AgNPs were varied from 24 h to day 14 to mimic the procedure employed in the analysis of the standard solutions presented earlier in this paper. The percent metal ion removed following the AgNP incubation were calculated using equation (2) above.

Table 4. Determination of the amounts of Fe^{2+} and Mn^{2+} ions in groundwater samples before treatment with AgNPs. Concentrations shown are the mean of 4 replicates with standard deviations within ±0.005 ppm

Sample sites	Fe/ppm	Mn/ppm
Kotokuraba	0.192	0.299
Efutu	0.255	0.267
Pedu	0.581	0.138
OLA	0.300	0.135
Assin Fosu	0.213	0.203

Table 5. Percentage removal efficiencies of AgNPs at various incubation periods. Shown in the table are the mean values of 4 replicates with standard deviations within ±0.04

Sample sites	Incubation days	% Fe	% Mn
Kotokuraba	1	6.26	3.28
	3	7.95	4.75
	5	14.40	4.82
	7	15.72	5.27
	14	22.69	6.42
Efutu	1	3.84	2.95
	3	11.19	7.64
	5	15.72	7.76
	7	26.82	9.41
	14	29.85	9.72
Pedu	1	16.64	7.28
	3	21.66	7.62
	5	40.94	7.88
	7	40.96	8.02
	14	41.02	9.52
OLA	1	2.22	6.42
	3	7.82	8.33
	5	10.30	9.47
	7	15.00	10.34
	14	15.45	11.50
Assin Foso	1	8.06	43.10
	3	9.02	44.73
	5	25.94	45.34
	7	26.15	45.78
	14	27.71	46.03

A closer look at the results presented in Table 5 reveals a number of interesting observations. Firstly, amount of metal ion adsorbed increases with longer incubation times consistent with the results presented earlier in this paper. This observation is also supported by an earlier research work carried out by Alissawi *et al* and Alqudami *et al* which showed that longer incubation period enhances maximum metal-ion removal (Alissawi *et al*., 2013; Alqudami *et al*., 2013). Secondly, amounts of iron (II) ions removed were relatively higher than those of manganese, except the results obtained from Assin Foso. The higher removal efficiencies recorded for the control samples from Assin Foso might contradict our earlier assertion that sea intrusions might not impact the measured concentrations. Thirdly, the NP removal efficiencies observed in the proof of concept experiment were higher than the ones recorded for groundwater samples taken from Cape Coast metropolis and Assin Foso. This observation might be attributed to the complex nature of groundwater samples. Again, these results suggest a further investigation into the adsorption characteristics of metal-ion onto NPs in groundwater samples and a possible application of surface modification schemes to enhance the nanoparticles removal efficiencies. Nonetheless, the nanoparticle removal efficiencies, though not as expected, are still quite substantial given the relative complexities of groundwater analysis. In a nutshell, this work has demonstrated to a greater extent the plausibility of applying unmodified nanoparticles in the removal of metal-ion contaminants from groundwater samples. It has opened up a new frontier of research into the use of nanoparticles in the treatment of groundwater sources.

CONCLUSION

This research presented herein has shown that silver nanoparticles are easy to synthesize, inexpensive due to low cost of materials used, do not produce sludge when used for water treatment, and have high metal-ion adsorption capacity as observed in the preceding chapters. It can also be concluded that AgNPs metal–ions adsorption begins just after incubation as shown in the sharp decrease from the spectral analysis as discussed earlier. In addition we can conclude that AgNPs efficiency towards metal-ion removal in complex solutions and other aqueous media is time–dependent. Also the nanoparticle removal efficiencies as observed in the proof of concept laboratory experiments were higher than groundwater samples taken from wells in Cape Coast and Assin Fosu. This observation might be attributed to the complex nature of groundwater samples. This could also mean that there were other substances and ions in the groundwater samples that the nanoparticle has more affinity for; hence adsorbed them leaving a less surface area for the target ions adsorption. This observed results suggest a thorough investigation into the adsorption characteristics of metal-ion onto nanoparticles in groundwater samples.

REFERENCES

Abdul Jameel, A., Sirajudeen, J. and Abdul vahith, R. 2012. Studies on heavy metal pollution of ground water sources between Tamilnadu and Pondicherry, India. *Advances in Applied Science Research,* 3(3), 424-429.

Alissawi, N., Zaporojtchenko, V., Strunskus, T., Kocabas, I. and Chakravadhanula, V. S. K. 2013. Effect of gold alloying on stability of silver nanoparticles and control of silver ion release from vapor-deposited Ag–Au/polytetrafluoroethylene nanocomposites. Gold Bull, 46(1), 3–11.

Alqudami, A., Munassar, S. and Alhemiary, N. 2013. The Sorption Properties of Exploding Wire Prepared Ag, Fe and ZnO Nanoparticles for Nitrite Removal from Water. International Journal of Material Science, 3(1), 18-25.

Ashutosh, A. and Himanshu, J. 2010. Application Of Nanotechnology In The Remediation Of Contaminated Groundwater: A Short Review. Recent Research in Science and Technology, 2(6), 51-57.

Ball, D. W. 2006. Field Guide to Spectroscopy (Vol. FG08 pp. 1-124). Bellingham, WA: SPIE Press.

Biziuk, M., Beyer, A. and Zukowska, J. 2010. Preservation and Storage of Water Samples. In J. Namiesnik and P. Szefer (Eds.), Analytical Measurements in Aquatic Environments. (pp. 19-39). London: CRC Press.

Ding, J., Di, Z., Wu, D., Luan, Z., Zhu, Y. and Li, Y. H. 2005. Adsorption thermodynamic, kinetic and desorption studies of Pb2+ on carbon nanotubes. Water Research, 39(4), 605-609.

Donald, D. A., Shugar, G. J., Shari, B. L. and Lauber, J. 2001. Environmental Field Testing And Analysis Ready Reference Handbook (pp. 1.31-32.140). New York: McGraw - Hill Inc.

Elangovan, R., Philip, L. and Chandraraj, K. 2008. Biosorption of hexavalent and trivalent chromium by palm flower (Borassus aethiopum). Chemical Engineering Journal, 141(1–3), 99-111.

Kogan, M. J., Bastus, N. G., Amigo, R., Grillo-Bosch, D., Araya, E., Turiel, A. and Puntes, V.F. 2006. Nanoparticle-Mediated Local and Remote Manipulation of Protein Aggregation. Nano Lett., 6, 110–115.

Monteagudo, J. M. and Ortiz, M.J. 2000. Removal of inorganic mercury from mine waste water by ion exchange. *Journal of Chemical Technology and Biotechnology*, 75(9), 767-772.

Pradeep, T. and Anshup, 2009. Noble metal nanoparticles for water purification. Thin Solid Films, 517(24), 6441–6478.

Shim, J. Y. and Gupta, V. K. 2007. Reversible Aggregation of Gold Nanoparticles Induced by pH Dependent Conformational Transitions of a Self-Assembled Polypeptide. *J. Colloid Interface Sci.,* 316, 977–983.

Solomon, S. D., Bahadory, M., Jeyarajasingam, A. V., Rutkowsky, S. A., Boritz, C. and Mulfinger, L. 2007. Synthesis and Study of Silver Nanoparticles. Journal of Chemical Education, 2(84), 322-325.

Standard Methods for the Examination of Water and Wastewater, 2005. (21st ed.). Washington DC: American Public Health Association (APHA), American Water Works Association (AWWA) and Water Environment Federation (WEF).

Suksabye, P., Thiravetyan, P. and Nakbanpote, W. 2008. Column study of chromium (VI) adsorption from electroplating industry by coconut coir pith. Journal of Hazardous Materials, 160(1), 56-62.

Sumesh, E., Bootharaju, M. S., Anshup, and Pradeep, T. 2011. A practical silver nanoparticle-based adsorbent for the removal of Hg2+ from water. *Journal of Hazardous Materials,* 189 (1-2), 450 – 457.

Sundaram, B., Feitz, A. J., Caritat, P. d., Plazinska, A., Brodie, R. S. and Coram, J. 2009. Groundwater Sampling and Analysis – A Field Guide (pp. 51). Australia: Geoscience.

Weng, C. H., Sharma, Y. C., and Chu, S.H. 2008. Adsorption of Cr (VI) from aqueous solutions by spent activated clay. *Journal of Hazardous Materials,* 155(1–2), 65-75.

Yang, K., Zhu, L. Z. and Xing, B. S. 2006. Adsorption of Polycyclic Aromatic Hydrocarbons by Carbon Nanomaterials. *Environmental Science and Technology,* 40(6), 1855-1861.

Yantasee, W., Warner, C. L., Sangvanich, T., Addleman, R. S., Carter, T. G. and Wiacek, R. J. 2007. Removal of Heavy Metals from Aqueous Systems with Thiol Functionalized Superparamagnetic Nanoparticles. *Environmental Science and Technology,* 41(14), 5114-5119.

****